

Electrokinetic properties of mineral mixtures

Jiří Škvarla¹

Elektrokinetické vlastnosti zmesí minerálov

Elektroforetický rozptyl svetla (ELS) je nová experimentálna technika umožňujúca merať spectrum elektroforetickej pohyblivosti alebo zeta (ζ) potenciálu skupiny častíc. Toto spectrum odráža distribúciu náboja a čiastočne distribúciu rozmeru týchto častíc. Avšak, okrem modálnej hodnoty napr. zeta potenciálu častíc rovnakého druhu, z ELS spektra môžeme vyčítať aj niektoré ďalšie charakteristiky disperzného systému. Pre vybrané binárne zmesi dobre definovaných koloidných a jemnozrnných častíc SiO₂ a SiO₂ modifikovaných aminopropylom alebo hematitu (tieto zložky majú odlišné charakteristiky povrchového náboja) boli z ELS spektier určené rozsahy pH vodného prostredia pri ktorých dochádza k heterokoagulácii, heterostabilizácii a heterokoagulačno-heterostabilnému prechodu týchto častíc. K úplnej heterokoagulácii dochádza ak (jediná) modálna hodnota monomodálneho ELS spektra zmesi leží medzi modálnymi hodnotami ELS spektier jednotlivých zložiek zmesi pri tom istom pH. Úplná heterostabilita sa naopak uplatňuje keď obidve modálne hodnoty bimodálneho ELS spektra zmesi sa zhodujú s modálnymi hodnotami ELS spektier zložiek pri rovnakom pH. Heterokoagulačno-heterostabilný prechod bol nakoniec identifikovaný v situácii keď pre zmes sa získalo bimodálne spectrum, avšak aspoň jedna jeho modálna hodnota bola odlišná od modálnej hodnoty ELS spektra niektorej zo zložiek. Takto odhadnuté charakteristiky boli potvrdené výpočtom energetickej bariéry medzi časticami-zložkami.

Kľúčové slová: Elektroforetický rozptyl svetla, zeta potenciál, heterokoagulácia, koloidy, elektrostatické povrchové sily

Introduction - the science of mineral processing and colloid (surface) interactions

J.A.Kitchener in his introductory overview in the book *Colloid Chemistry in Mineral Processing* states: "The term mineral processing is mainly associated with techniques for extracting valuable minor components from mined rocks – for example, a few percent of galena, PbS, from an ore containing also small amounts of sphalerite, ZnS, pyrite, FeS, etc., embedded in a major proportion of a silicate gangue. Nowadays processing of one kind or another is also applied to a variety of industrial minerals, even such bulk materials as coal and clays" (Kitchener, 1992). This general characterization of mineral processing, relying upon mechanical or physical methods of separation such as jigging, heavy media, magnetic, electrostatic or optical sorting, has to be extended: "Since the size of the particles which are currently processed is rapidly approaching colloidal range, mineral processing is, of necessity, becoming more and more an applied colloid chemistry" (Laskowski and Ralston, 1992, foreword). Kitchener further detail the role of colloid chemistry in mineral processing: "There are three areas where colloid-chemical effects come into play: (1) The separation of very small grains of mixed minerals which have resulted from fine grinding of an ore (generally by crushing and ball-milling) in order to liberate the individual mineral species; (2) The "beneficiation" of minerals which occur naturally in microparticle form, notably the more valuable clays; (3) The control of waste slurries, muds, etc., which must not be allowed to pollute the environment. All three depend on surface properties ... surface effects become increasingly prominent... as particle size decreases" (Kitchener, 1992).

Hence, on the one hand, the objective of mineral processing is unceasingly to selectively separate mixed fine or even colloidal particles of various minerals, irrespective of whether comminuted, natural or waste. On the other hand, mutual surface interactions (heterointeractions) always operate between different particles that may make the selective separation difficult or impossible.

Selective separation and surface forces – heterocoagulation

To explain the problem of selective separation due to the surface heterointeractions, the following paragraph of Kitchener can be also adopted: "It might be supposed that the minerals in an ore would be mutually in equilibrium, having remained in close proximity for millions years. But fine-grinding of an ore in water may set off new processes through dissolution, hydrolysis, adsorption, oxidation or colloidal interactions. The active surfaces of freshly crushed crystals may adsorb ions from slightly soluble constituents; for example: a trace of Pb coming from oxidizing galena may be sufficient to activate silicates towards flotation reagents. A trace of hydrolyzing Fe ions, coming from steel grinding balls, has been known to depress the zeta potential of quartz and colloidal ferric oxide readily deposits onto sulphide mineral grains" (Kitchener, 1992). Apparently, surface forces operating between different particles and causing their heteroaggregation or heterocoagulation (opposed to heterostability) are of a special importance. The heterocoagulation process is naturally evoked by the attractive

¹ Doc. Ing. Jiří Škvarla, CSc., Katedra mineralurgie a environmentálnych technológií, Fakulta BERG Technickej univerzity v Košiciach, Park Komenského 19, 043 84 Košice
(Recenzované a revidované verzia dodaná 14.7.2003)

electrostatic surface force between dissimilar electrical double layers (more strictly between their diffuse parts), established around particles as a consequence of their surface charge generation (we should remember that in mineral suspensions there are various oxides, sulfides, carbonates, etc., having different mechanisms of the surface charge generation). There are two limit situations; oppositely charged particles attract each other, forming heteroaggregates, while equally charged particles (with the same sign and magnitude of the surface charge) are mutually repelled, remaining heterostable. As an example of the electrostatically-driven heterocoagulation, we can mention the slime coating where fine slime clay particles, usually carrying a negative surface charge, are attracted to positively charged larger mineral grains (Kitchener, 1992). But, the situation when particles possess charges of the same sign but different magnitude is also possible; in this case, the electrostatic surface force is more complex and heterostability or heteroaggregation can occur in principle depending on the absolute magnitudes of the surface charges.

Electrical double layer and electrophoresis

Particles immersed in a polar liquid medium like water acquire a surface charge. At the same time, this charge can arise, as anticipated previously, in many different ways. The most important mechanism of the surface charge generation is that via ionisation of surface functional groups: if a surface contains acidic functional groups, their dissociation gives rise to a negatively charged surface, conversely, a basic surface takes on a positive charge. In both cases the magnitude of the surface charge, i.e. the degree of surface ionisation, depends on the acidic or basic strength of the surface functional groups and on pH of the solution. The surface charge can be reduced to zero (at the point of zero charge, PZCH) by suppressing the surface ionisation by decreasing pH in the former case or by increasing pH in the latter case. Metal oxides, carrying hydroxyl surface functional groups, exhibit the amphoteric behaviour and both positively and negatively charged surface can be obtained by varying pH. The electrically charged surface is physically unstable and tend to be neutralized. To neutralize the overall positive or negative surface charge, oppositely charged ions (counterions) are electrostatically attracted to the surface from the solution while equally charged ions (coions) are repelled from that surface to the solution, both attaining an equilibrium between their electromigration and thermal diffusion motion. The asymmetrical distribution of the electrolyte ions at the interface results in the establishment of the electrical double layer (EDL) that consists of the inner (Stern) layer associated with the adsorbed counterions and the diffuse (Gouy) layer of the rest of counterions and all coions.

When placed in the electric field, a particle will move due to its surface charge toward the electrode of opposite charge. This phenomenon is called electrophoresis. The situation, however, is complicated since the EDL neutralizing the surface charge is regularly built up around the particle. Consequently, the electrical double layer of the particle is forced to split up, rendering its rigid (adjacent to the interface) part moving electrophoretically together with the particle and a mobile (distant from the interface) part traveling in the reverse direction. The plane of the "shear" is extended out from the particle surface and separates the so-called electrokinetic or hydrodynamic unit, that moves as a single entity, from the bulk of the solution. In principle, the dry particle size is less than the hydrodynamic size of the kinetic unit. However, the difference is obviously very small. In fact, the exact location of the shear plane cannot be defined but it is agreed to be somewhere beyond the limit of the Stern layer so that the so-called zeta (ζ) or electrokinetic potential at the shear plane is a bit lower than the Stern (φ_s) potential. The experimentally measured drift electrophoretic velocity of the electrokinetic unit v_c (in $\text{m}\cdot\text{s}^{-1}$) is proportional to the electric field strength (unit field gradient), E ($\text{V}\cdot\text{m}^{-1}$), with the proportionality constant called electrophoretic mobility, μ_c ($\text{m}^2\cdot\text{s}^{-1}\cdot\text{V}^{-1}$):

$$v_c = \mu_c E \quad (1)$$

The zeta potential can be calculated from the electrophoretic mobility using two models representing limits of the Henry's equation, namely the Smoluchowski and the Hückel limit, according to the dimensionless product κa :

$$\mu_c = (\varepsilon\zeta/\eta) \quad \text{for } \kappa a \gg 1 \text{ (Smoluchowski limit)} \quad (2)$$

$$\mu_c = (2\varepsilon\zeta/3\eta) \quad \text{for } \kappa a \ll 1 \text{ (Hückel limit)} \quad (3)$$

where a is the radius of the electrokinetic unit (particle), κ is the reciprocal diffuse layer width (Debye length), ε is the permittivity (dielectric constant) and η is the dynamic viscosity of the liquid medium. For particles in aqueous solutions it is impossible to satisfy the Hückel limit and it is not easy to completely satisfy the Smoluchowski limit either. The argument is that most particles range in size from 100 to 1000 nm so that in an aqueous electrolyte solution such as 10^{-3} M KCl ($\kappa = 0,1 \text{ nm}^{-1}$), κa will vary from 10 to 100. However, for particles in a real water, κa is higher and the Smoluchowski limit is generally more appropriate for the

conversion of the electrophoretic mobility to the zeta potential. In this limit, the zeta potential (mV) in water at 25°C is related to the electrophoretic mobility ($\mu\text{m}\cdot\text{s}^{-1}\cdot\text{V}^{-1}\cdot\text{cm}$ or $10^{-8}\text{m}^2\cdot\text{s}^{-1}\cdot\text{V}^{-1}$) as follows:

$$\zeta = 12.83\mu_e \quad (4)$$

The range of the electric field strength is from near 0 to a few tens of V/cm. The electrophoretic velocities that develop are in the range of 0 to a few hundred $\mu\text{m}/\text{s}$. Mobilities are in the range of 0 to $\pm 10\ \mu\text{m}\cdot\text{s}^{-1}\cdot\text{V}^{-1}\cdot\text{cm}$ and zeta potentials will not exceed ± 100 mV as a rule.

Electrophoretic light scattering – principles and features

When a charged particle electrophoretically moves perpendicularly to an incident laser beam direction, the frequency of light scattered by this particle is shifted. This so-called (angular) Doppler shift in the frequency of the scattered light, ω_s , is given by the dot product:

$$\omega_s = \mathbf{q}\cdot\mathbf{v}_e = q\cdot v_e\cdot\cos(\theta/2) \quad (5)$$

where \mathbf{q} and q is the scattering vector and its magnitude, respectively. Similarly, \mathbf{v}_e and v_e is the electrophoretic velocity vector and its magnitude, respectively. θ is the scattering angle between the incident laser beam and the particle-detector line. The scattering vector magnitude is given as:

$$q = (4\pi n/\lambda_0)\sin(\theta/2) \quad (6)$$

where n is the refractive index of the liquid medium λ_0 is the wavelength of the laser beam in vacuum. By combining Eq. (5), (6) and (1), we obtain:

$$\omega_s = (4\pi n\mu_e E/\lambda_0)\sin(\theta/2)\cos(\theta/2) \quad (7)$$

When taking $n = 1.322$ for water in the red end of the visible range of wavelengths, $\lambda_0 = 670$ nm and $\theta = 15^\circ$ one can relate the Doppler shift frequency to the electrophoretic mobility (and zeta potential):

$$\omega_s = 3.22\cdot\mu_e\cdot E \quad (\text{rad}\cdot\text{s}^{-1}) \quad (8)$$

or

$$v_s = \omega_s/2\pi = 0.513\cdot\mu_e\cdot E \quad (\text{Hz}) \quad (9)$$

where E is in units of V/cm and μ_e in $\mu\text{m}\cdot\text{s}^{-1}\cdot\text{V}^{-1}\cdot\text{cm}$. A reasonable approximation for the maximum of the product $\mu_e\cdot E$ is 400 $\mu\text{m}/\text{s}$. Then a maximum Doppler shift v_s is 200 Hz.

At the first sight, all particles in a monodisperse system should move electrophoretically with the same mobility and so scatter light with the same Doppler shift frequency. However it is a distribution of Doppler shift frequencies with a characteristic modal frequency what is regularly measured due to the inherent surface charge heterogeneity of particles (Weiner et al., 1993). Hence, the resultant signal of the electrophoretic light scattering (ELS), as this special embodiment of both laser-Doppler velocimetry (LDV) and quasielastic light scattering (QELS) is named, is a complete Doppler shift frequency, electrophoretic mobility or zeta potential histogram (generally ELS spectrum). The principal advantage of ELS is a fast (many thousand times faster than conventional microelectrophoretic techniques) collection of the ELS spectra. On the other hand, despite of the advantage of simple illumination, optics and signal processing, ELS has also limitations inherent in light scattering. First, ELS spectra may be additionally broadened due to Brownian diffusion of particles. In general, particles diffuse translationally with velocities of magnitude higher than the electrophoretic drift velocities at the usual electric field strength. Thus, the Doppler shift frequencies should primarily depend upon the abrupt thermal motions of particles rather than upon their electrophoresis. However, the frequency of scattered light can be affected only by motions which carry particles a substantial fraction of the wavelength of the illuminating light and individual steps in the random walk executed by particles are small (a few angströms) to be detectable with light of optical wavelength. Therefore, only cumulative effects of many random steps are detectable, as the diffusional broadening (Ware and Haas, 1983), without influencing the modal Doppler shift frequency. The Lorentzian linewidth (half width at half height) of an ELS spectrum Γ is proportional to the parameter q and the translational diffusion coefficient D_T of particles:

$$\Gamma = D_T\cdot q^2 \quad (10)$$

Therefore, the diffusional broadening is inversely proportional to the particle size because $D_1 = kT/6\pi\eta a$. Also it is proportional to the scattering angle via q . In water at 25°C and $\lambda_0 = 670$ nm, Eq. (10) becomes $\Gamma_{15} = 414/a$ and $\Gamma_{90} = 12000/a$ (Γ in Hz and a in nm). As we can see, at low scattering angles such as 15°, $\Gamma_{15} < 10$ Hz for $a > 50$ nm and $\Gamma_{15} < 1$ Hz for $a > 500$ nm.

The second cause of broadening ELS spectra is particle size heterogeneity (polydispersity). Among other effects that can broaden ELS spectra, thermal effects are the most significant. The argument is that the electric field E at any point in the solution is a function of the conductivity of the solution at that point, and of the electrical current density flowing through that region, as predicted by the microscopic version of the Ohm's law:

$$E = I/B \cdot \sigma \quad (11)$$

where σ is the conductivity, I is the ionic electrical current and B is the cross-sectional area through which the current flows in the vicinity of interest. As a consequence, the inevitable Joule heating generated by regions conducting electrical current will cause the solution temperature to increase, engendering a few peak broadening phenomena (Ware and Haas, 1983). The most important Joule-heating-related broadening is caused by the fact that the solution viscosity η decreases, thereby increasing the particles' electrophoretic mobilities during the course of the observation [Eq.(2) and Eq.(3)]. This first-order phenomenon can be minimized by establishing the electric field with a constant-current power supply instead of a constant-voltage power supply.

Electrophoretic light scattering and heterocoagulation-heterostability transition

As mentined above, the electrostatic surface force between particles causes their heterocoagulation or heterostability depending on the sign and absolute magnitudes of the surface charges of these particles. Since H^+ ion determines the surface charge of most particles, pH has widely been chosen to be the main factor regulating heterocoagulation and heterostability. According to theories of the electrostatic surface force, spontaneous heterocoagulation occurs at pH where particles carry surface charges of opposite sign, i.e. between their isoelectric points, an electrostatic barrier arises whose height depends on the absolute magnitudes of the surface charges, causing heterocoagulation due to the attractive electrostatic surface force to be metastable. If pH above isoelectric points and surface charges are such that the electrostatic barrier is high enough, the particles may be completely prevented from heterocoagulation, i.e. they are heterostable. Table 1 summarizes the pH range of heterocoagulation and heterostability published for various binary colloidal and fine mineral mixtures. These mixtures are divided into three categories, depending on a degree of their particles' characterization: (i) *Category 1 (well characterized particles): Synthetized spheres with a low size heterogeneity*; (ii) *Category 2 (moderately characterized particles): Syntetized or natural mineral particles with a high size heterogeneity*; (iii) *Category 3: Mineral "complexes"* (i.e. systems where at least one component is not a true solid phase). As one can see from Table 1, light scattering, sedimentation, SEM and TEM are the most frequently used techniques for evaluating the pH-regulated heterocoagulation and heterostability phenomena in binary mixtures. Nevertheless, no experiments have been published evaluating pH of the heterocoagulation-heterostability transition directly in the mixture.

It has been shown that two or more kinds of heterostable particles, from spheres of different polymer latexes (Xu, 1993; McNeil-Watson, 1991) to ceramic particles of titania and alumina (Jia and Williams, 1990), coexisting in a mixture provide a bimodal ELS spectrum having the peak positions to be identical with the peak positions of monomodal ELS spectra taken separately for the respective kinds of particles. This means heterocoagulation is absent. On the other hand, if an electrophoresing particle undergoes a chemical reaction which changes that particle's charge and/or size, the particle abruptly changes its velocity; therefore any chemical reaction will perturb an ELS spectrum if its time scale is on the order of the spectral time scale (Ware and Haas, 1983). Similarly, heterocoagulation, if fast enough, should be detected in ELS spectra since the surface charge of heterocoagulates differs from these of individual particles incorporated in them.

Really, the formation of heterocoagulates in binary mixtures has been manifested in their ELS spectra, differing from these expected by superimposing monomodal ELS spectra of individual components (Škvarla, 1996a,b). To illustrate how the pH-induced heterocoagulation-heterostability transition can be evaluated using the ELS technique, ELS spectra of various binary mixtures were measured at varying pH. We recorded the zeta potential (ζ) spectra provided by diluted colloidal mixtures of pure silica spheres and silica spheres with surface-introduced aminopropyl in distilled water (no supporting electrolyte was added in order to maximize the surface charge) as a function of pH (not shown here). The silica spheres are well characterized so that their mixtures can be considered as of the category 1. The ζ -spectra were monomodal (as expected for the one-component systems), with no shoulders. For example, at pH 7.3 the peak position, i.e. the modal value of ζ was -41.5 mV and -22.4 mV for silica and silica/aminopropyl, respectively. Fig. 1 shows the complete dependence of the modal ζ on pH for both individual silicas. After their mixing, different ζ -spectra were observed depending on pH: bimodal at pH 6.6 to 8.3 and monomodal at pH 6.2. Both modal ζ 's of bimodal ζ -spectra provided by single silica and

Tab.1. pH range of heterocoagulation and heterostability published for various colloidal and fine mineral mixtures.
 Tab.1. pH rozsah heterokoagulácie a heterostability publikovaný pre rôzne koloidné a jemnozrnné minerálne zmesi.

Component 1	Component 2	Heterocoagulation pH range	Heterostability pH range	method	reference
Category 1: Synthetized spheres with a low heterogeneity					
<i>anionic polystyrene (sulfate) latex (PS)</i> $a = 159 \text{ nm}$ no pH_{IEP} $c = 10^{-3} \text{ M KNO}_3, N_0 = 10^{14} \text{ m}^{-3}$	<i>cerium (hydrous) oxide</i> $a = 110 \text{ nm}$ $\text{pH}_{\text{IEP}} = 6.8$	$\leq 6.6^a$	≥ 9.0	Light scattering	Kihira and Matijevec, 1992
<i>polyvinyl chloride latex (PVC)</i> $a = 169 \text{ nm}$ no pH_{IEP} $c = 8.9 \times 10^{-3} \text{ M NaNO}_3$	<i>chromium hydroxide ($\text{Cr}(\text{OH})_3 \cdot \text{H}_2\text{O}$)</i> $a = 186 \text{ nm}$ $\text{pH}_{\text{IEP}} \sim 7.4$	≤ 6.0	≥ 9.0	Light scattering	Bleir and Matijevec, 1976
<i>polytetrafluoroethylene latex (PTFE)</i> no pH_{IEP} $c = 10^{-2} \text{ M}, N_0 = 1.2 \times 10^{18} \text{ m}^{-3}$	<i>hematite ($\alpha\text{-Fe}_2\text{O}_3$)</i> $a = 25 \text{ nm}$ $\text{pH}_{\text{IEP}} = 6.0$	≤ 6.0	≥ 6.5	Sedimentation	
TiO_2 $a = 45 \text{ nm}$ $\text{pH}_{\text{IEP}} = 5.9$ $c = 10^{-4} \text{ M KNO}_3, 50 \text{ and } 100 \text{ mg/l TiO}_2, 150 \text{ and } 300 \text{ mg/l Al}_2\text{O}_3$	Al_2O_3 $a = 10 \text{ nm}$ $\text{pH}_{\text{IEP}} = 8.9$	5.6 - 8.9	≥ 9.0	Light scattering	Wiese and Healy, 1975a,b,c,d; Healy et al., 1973
<i>anionic sulfate latex (RP)</i> $a = 150 \text{ nm}$ $N_0(\text{RP} + \text{JA3}) = 2.5 - 6 \times 10^{16} \text{ m}^{-3}$	<i>cationic amide latex (JA3)</i> $a = 90 \text{ nm}$ $\text{pH}_{\text{IEP}} = 9 - 10$	$\leq 10^b$	≥ 12	Light scattering	Maroto and de las Nieves, 1995
<i>sulfate polystyrene latex</i> $a = 83.5 \text{ nm}$ $c = 0 - 10^{-1} \text{ M NaNO}_3, N_0(\text{total}) = 5 - 7.2 \times 10^{15} \text{ m}^{-3}$	<i>amidine polystyrene latex</i> $a = 48.5 \text{ nm}$	determined only at pH 5.7		Light scattering	Ryde and Matijevec, 1994
<i>anionic polystyrene latices (PS)</i> $a = 90, 160 \text{ and } 348 \text{ nm};$ <i>anionic polyvinylidene-chloride latex (PVDC)</i> $a = 58 \text{ nm}$ $c = 10^{-5} - 5 \times 10^{-3} \text{ M KCL}, N_0 = 2.7 - 8.03 \times 10^{15} \text{ m}^{-3}$	<i>cationic polystyrene latices (PS)</i> $a = 1,085 \text{ nm}$	determined only at pH 6.0		SEM	Harley et al., 1992
<i>silica (SiO_2)</i> $a = 35 \text{ nm}$ $\text{pH}_{\text{IEP}} = 3.1$ $c = 10^{-2} \text{ M NaNO}_3, 50 \text{ mg/l SiO}_2, 21.3 \text{ mg/l } (\alpha\text{-Fe}_2\text{O}_3)$	<i>hematite ($\alpha\text{-Fe}_2\text{O}_3$)</i> $a = 70 \text{ nm}$ $\text{pH}_{\text{IEP}} = 7.9$	3.0, 4.0, 5.5, and 10.0		Light scattering and Zeta potential	Esumi et al., 1998
<i>silica (SiO_2)</i> $a = 120, 230, 480 \text{ and } 795 \text{ nm}$ $\text{pH}_{\text{IEP}} = 3.2$ $c = 10^{-5} \text{ M KCL}, 5\% \text{ wt. SiO}_2$	<i>amphoteric polymer</i> $a = 125 \text{ nm}$ $\text{pH}_{\text{IEP}} = 7.2$	3.0 - 4.5		SEM and Sedimentation	Furusawa and Anzai, 1992

Category 2: Synthetized or natural mineral particles with a high size heterogeneity

<i>quartz (SiO₂)</i> <i>a</i> = 50 - 200 nm pH _{IEP} = 2.0 <i>c</i> = 0.22 % wt SiO ₂ + TiO ₂	<i>rutile (TiO₂)</i> <i>a</i> = 100 nm pH _{IEP} = 4.5	2.0 - 5.6 ^c	≥ 7.0	Sedimentation	Pugh, 1992
<i>quartz (SiO₂)</i> <i>a</i> = 50 - 200 nm pH _{IEP} = 2.0 <i>c</i> = 0.22 % wt SiO ₂ + (α-Fe ₂ O ₃)	<i>hematite (α-Fe₂O₃)</i> <i>a</i> = 50 - 200 nm pH _{IEP} = 6.2	≤ 7.0 ^d	≥ 8.0	Sedimentation	Pugh, 1992
<i>α-SiC</i> <i>a</i> = 900 nm pH _{IEP} = 2.4 <i>c</i> = 10 ⁻³ M KCL, 0.5% vol. α-SiC + α-Si ₃ N ₄	<i>α-Si₃N₄</i> <i>a</i> = 250 nm pH _{IEP} = 6.5	≤ 7.0	≥ 7.5	Sedimentation	Wilson and Crimp, 1993
<i>quartz (SiO₂)</i> <i>a</i> < 5 mm pH _{IEP} = 2.2	<i>hematite concentrate</i> <i>a</i> < 5 mm pH _{IEP} = 5.3	≤ 5.3 ^e	≥ 6.5	HGMS	Wang et al., 1992
<i>NH₄-montmorillonite</i> <i>a</i> = 23 nm no pH _{IEP} N _o (total) ≤ 4.35x10 ¹⁸ m ⁻³ (≤1gf ⁻¹)	<i>Fe-oxyhydroxide (akaganeite)</i> with minor impurities (<i>lepidocrocite, goethite</i>) <i>a</i> = 30 nm pH _{IEP} = 2.4	determined only at pH 3.2 -5.8	-	Light scattering	Ferreiro et al., 1995

Category 3: Mineral „complexes“

<i>gold</i> <i>a</i> = 6 nm <i>c</i> = 10 ⁻² and 10 ⁻¹ M NaNO ₃	<i>goethite (α-FeO.OH)</i> pH _{IEP} = 7.2	determined only at pH 5.6	≥ 7.0	TEM	Enzweiler and Joekes, 1991, 1992
<i>kaolinite</i> pH _{IEP} = 7.2 <i>bentonite</i> and <i>illite</i> no pH _{IEP}	<i>amorphous Fe (III) hydroxide</i> pH _{IEP} = 5.4 - 6.7	determined only at pH 5.6	determined only at pH 5.6	TEM and Zeta potential	Ohtsubo, 1989; Yong and Ohtsubo, 1987
<i>70% illite + small amount of kaolinite</i> no pH _{IEP} <i>c</i> = 5x10 ⁻³ M NaCL, 8%(wt)	poorly crystallized akaganeite (<i>β-Fe₂O₃</i>) pH _{IEP} = 6.4 - 8.4	determined only at pH 3.0	determined only at pH 9.5	TEM	Ohtsubo et al., 1991

^achromium hydroxide homocoagulates at pH 6 - 9

^bJA3 latex homocoagulates at pH 10 - 11

^crutile homocoagulates at pH 5.6

^dhematite homocoagulates at pH 7 - 7.5

^ehematite concentrate homocoagulates at pH 5.3 - 6.5

Tab.2. $E^{EL}(max)$ calculated for the silica-silica/aminopropyl and silica-hematite mixtures after Eq.(12).
 Tab.2. $E^{EL}(max)$ vypočítané pre SiO_2 - SiO_2 /aminopropyl a SiO_2 -hematit zmesi podľa rovnice (12).

pH	$\psi_{Si}(mV)^*$	$\psi_{Si_2}(mV)^*$	$E^{EL}(max)/kT$	ELS prediction
<u>silica-silica/aminopropyl system</u>				
6,2	-36,5	~0	-	heterocoagulation
6,6	-37,0	-7,7	7	transition
6,9	-41,1	-15,8	35	heterostability
7,3	-41,5	-22,4	93	heterostability
7,5	-42,6	-25,8	120	heterostability
7,6	-43,3	-33,7	199	heterostability
7,9	-49,9	-42,5	315	heterostability
8,3	-52,3	-53,2	495	heterostability
<u>silica-hematite system</u>				
5,7	-20,9	-7,9	7	heterocoagulation
6,1	-24,4	-12,2	9	heterocoagulation
6,4	-27	-14,2	27	heterocoagulation
7,2	-34,8	-17,2	43	transition
7,6	-35,4	-16,4	44	heterostability
8	-38,5	-16,5	32	transition
8,6	-39,2	-16,1	29	transition

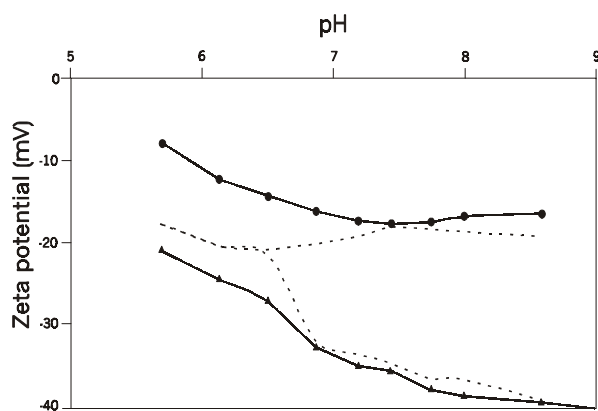


Fig.1. Modal ζ -potential of monomodal ELS ζ -spectrum for individual silica (lower full line), individual silica/aminopropyl (upper full line) and of the bimodal ζ -spectrum for their mixture (dashed lines) as a function of solution pH.

Obr.1. Modálny ζ -potenciál monomodálneho ELS ζ -spektra individuálnych častíc SiO_2 (spodná plná línia), SiO_2 /aminopropylu (horná plná línia) a bimodálneho ELS ζ -spektra ich zmesi (čiarkované línie) ako funkcia pH prostredia.

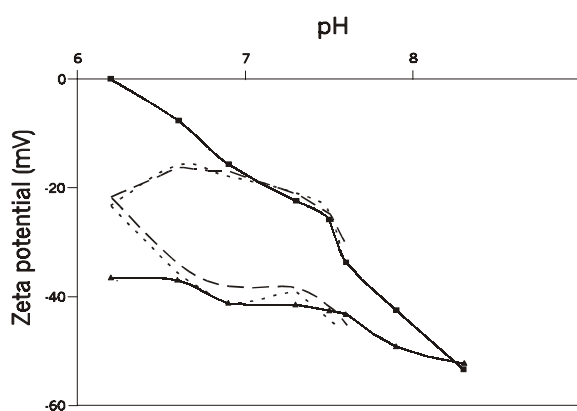


Fig.2. Modal ζ -potential of monomodal ζ -spectrum for individual silica (lower full line) and individual hematite (upper full line) and of the bimodal ζ -spectrum for silica-hematite mixture (dashed line) as a function of solution pH.

Obr.2. Modálny ζ -potenciál monomodálneho ELS ζ -spektra individuálnych častíc SiO_2 (spodná plná línia), hematitu (horná plná línia) a bimodálneho ELS ζ -spektra ich zmesi (čiarkovaná línia) ako funkcia pH prostredia.

silica/aminopropyl at the same pH whereas the modal ζ of the monomodal ζ -spectrum provided by the silica-silica/aminopropyl mixture at pH 6.2 was between these of monomodal ζ -spectra provided by single silica and silica/aminopropyl at the same pH. Only at pH 6.6 a specific situation occurred when the bimodal ζ -spectrum was taken for the silica-silica/aminopropyl mixture with the silica/aminopropyl modal ζ other than that of single silica/aminopropyl. To illustrate the above findings, the modal ζ 's of the bimodal and monomodal ζ -spectra provided by the silica-silica/aminopropyl mixtures as a function pH are depicted in Fig. 1 at two different ratios of silica to silica/aminopropyl particle concentration, viz 40 (long-dashed lines) and 80 (short-dashed lines). One can clearly see the deviation of the modal ζ 's from these of individual silicas at pH < 6.9. On the given time scale of minutes, the explanation can be as follows. Since both silica and silica/aminopropyl spheres in their mixtures are detected by ELS as „unmodified“ at pH \geq 6.9, they can be considered to be heterostable in this pH range. On the contrary, at pH 6.2 a complete heterocoagulation occurs as only silica-silica/aminopropyl heterocoagulates are detected by ELS, with pH 6.2 – 6.9 to be a heterostability-heterocoagulation transition range. It should be noted that no homocoagulation is detected by ELS. It is important to note that both silicas' peak broadening due to the Brownian diffusion was minimal ($\theta = 15^\circ$) to maximize the peak separation capability of the ELS measurements. Moreover, since the peak width measured (typically \approx 5 Hz) corresponded with Γ calculated after

Eq.(10), the surface charge heterogeneity was probably low. To support the above explanation, the energy maximum due to the electrostatic surface force between silica (1) and silica/aminopropyl (2) spheres has been calculated (Table 2) at selected pH's according to the formula of Bleier and Matijevic (1976):

$$E^{\text{EL}}(\text{max}) = (\pi\epsilon\epsilon_0 a/2)(\varphi_{\text{S1}}^2 + \varphi_{\text{S2}}^2)[(1+2/R)\ln(1+2/R) + (1-2/R)\ln(1-2/R)] \quad (12)$$

where $R = \varphi_{\text{S1}}/\varphi_{\text{S2}}$ ($\varphi_{\text{S1}} > \varphi_{\text{S2}}$), $a = 2a_1a_2/(a_1 + a_2)$. In this formula, derived from the HHF (Hogg et al., 1996) expression of the electrostatic interaction between dissimilar spheres (based on the linear approximation of the Poisson-Boltzmann equation), Stern potentials were replaced by zeta potentials measured for single silica and silica/aminopropyl. From Table 2 follows that the heterocoagulation-heterostability transition is predicted at pH 6.6 where $E^{\text{EL}}(\text{max})$ was calculated to be only 7 kT , in accordance with the ELS observation. This would mean that heterocoagulation occurs in the so-called primary minimum (no secondary minimum was calculated to exist even when van der Waals attraction was accounted for). The heterostability predicted by the ELS observation to occur at pH > 6.9 is theoretically justified as the calculated $E^{\text{EL}}(\text{max}) > 35 kT$. Since $\varphi_{\text{S2}} = 0$, $E^{\text{EL}}(\text{max})$ ceases at pH < 6.2, allowing the heterocoagulation.

Interestingly, two heterocoagulation-heterostability transition have been observed in the silica-hematite mixture. Fig. 2 shows the relationship between the modal ζ of the monomodal ζ -spectrum for both individual components and pH. As in Fig. 1, inserted is also the relationship between the modal ζ 's of the bimodal ζ -spectra obtained for the silica-hematite mixture. Comparing both relationships we can see a disagreement at pH < 7.5 and pH > 7.7. The first heterocoagulation-heterostability transition is expected at pH 6.5 to 7.5. Complete heterocoagulation should occur at pH < 6.5. The second heterocoagulation-heterostability transition is expected at pH > 7.7 where the modal ζ 's of the bimodal ζ -spectra obtained for the silica-hematite mixtures also differ from these obtained for single silica and hematite. Heterostability is expected only at pH 7.5 – 7.7. This seemingly unreal trend is again confirmed by calculations of $E^{\text{EL}}(\text{max})$. In the silica-hematite system, however, hematite particles were far from uniform spheres (as silica spheres) so that the value of their radius could not be inserted in Eq. (12). But, assuming that most of hematite particles are appreciably bigger than the silica spheres. Therefore, to obtain $E^{\text{EL}}(\text{max})$ for the sphere-plate interaction configuration, Eq. (12) is simply multiplied by the factor 2, considering the parameter a in Eq. (12) to be the silica sphere radius. Anyway, although not precise in its absolute value, calculated $E^{\text{EL}}(\text{max})$ followed the observed heterocoagulation/heterostability trend. The maximal $E^{\text{EL}}(\text{max})$ was calculated at pH 7.6 where full heterostability was really observed. By diminishing or rising pH, $E^{\text{EL}}(\text{max})$ decreases. This decrease is more pronounced in the former case when the heterocoagulation-stability transition at the pH range 6.5 – 7.5 is followed by full heterocoagulation at pH < 6.5; in the later case, only the (second) heterocoagulation-heterostability transition occurs at pH > 7.7. It is worth to mention that the maximal variation of the calculated $E^{\text{EL}}(\text{max})$ in this system for the studied pH scale is only 37 kT which value is small in comparison with that for the silica-silica/aminopropyl system (hundred kT).

The situation is complicated when mixtures consist of polydisperse mineral particles. For example, although individual quartz and magnesite dispersion provided a monomodal ζ -spectrum at pH from 7.4 to 11.25, with isoelectric point at pH < 3 (quartz) and 9.4 (magnesite), ζ -spectra of their mixtures had surprisingly three (or even four) peaks so that the procedure of determining the heterocoagulation-heterostability is not as reliable as for the above well-characterized systems. Also, the applications of Eq. (12) is limited. Nevertheless, bimodal ζ -spectra with the modal ζ 's identical with these of the monomodal ζ -spectra of individual minerals have been detected at least at pH > 10.5 (Škvarla, 1996b).

References

- BLEIER, A. and MATIJEVIC, E.: Heterocoagulation I. Interactions of monodispersed chromium hydroxide with polyvinyl chloride latex. *J. Colloid Interface Sci.* 55, 1976, pp.510-524.
- ENZWEILER, J. and JOEKES, I.: Adsorption of colloidal gold on colloidal iron oxides. *J. Geochem. Explor.* 40 1991, pp.133-142.
- ESUMI, K., IDOGAVA, H. and MEGURO, K.: Mixed colloidal dispersion of silica and hematite. *Bull. Chem. Soc. Jpn.*, 61, 1988, pp.2287-2290.
- FERREIRO, K., HELMY, A.K. and de BUSSETI, S.G.: Interaction of Fe-oxyhydroxide colloidal particles with montmorillonite. *Clay Minerals*, 30, 1995, pp.195-200.
- FURASAWA, K. and ANZAI, Ch.: Heterocoagulation behaviour of polymer latices with spherical silica. *Colloids Surfaces*, 63, 1992, pp.103-111.
- HARLEY, S., THOMPSON, D.W. and VINCENT, B.: The adsorption of small particles onto larger particles of opposite charge. Direct electron microscope studies. *Colloids Surfaces*, 62, 1992, pp.163-176.
- HEALY, T.W., WIESE, G.R., YATES, D.E. and KAVANAGH, B.V.: Heterocoagulation in mixed oxide colloidal dispersions. *J. Colloid Interface Sci.*, 42, 1973, pp.647-649.

- HOGG, R., HEALY, T.W. and FUERSTENAU, D.W.: Mutual coagulation of colloidal dispersions. *Transactions of the Faraday Society*, 62, 1966, pp.1638-1657.
- JIA, X. and WILLIAMS, R.A.: Particle deposition at a charged solid-liquid interface. *Chem. Eng. Comm.*, 91, 1990, pp.127-198.
- KIHARA, H. and MATIJEVIC, E.: Kinetics of heterocoagulation. 3. Analysis of effects causing the discrepancy between the theory and experiment. *Langmuir*, 8, 1992, pp.2855-2862.
- KITCHENER, J.A.: Minerals and surfaces. In: J.S. LASKOWSKI and J. RALSTON (Editors), *Colloid Chemistry in Mineral Processing*. Elsevier, Amsterdam, 1992, pp.1-35.
- LASKOWSKI, J.S. and RALSTON, J.: Foreword. In: J.S. LASKOWSKI and J. RALSTON (Editors), *Colloid Chemistry in Mineral Processing*. Elsevier, Amsterdam, 1992, pp. v-vii.
- MAROTO, J.A. and de las NIEVES, F.J.: Optimization of the heterocoagulation process of polymer colloids with different particle size. *Colloids and Surfaces*, 96, 1995, pp.121-133.
- McNEIL-WATSON, F. and PARKER, A.: Improvements in electrophoretic mobility measurements using laser-Doppler techniques. In: R.A. WILLIAMS and N.C. de JAEGER (Editors), *Advances in Measurement and Control of Colloidal Processes*, Butterworth Heinemann Ltd, Oxford, 1991, pp.122-135.
- OHTSUBO, M.: Interaction of iron oxides with clays. *Clay Sci.*, 7, 1989, pp.227-242.
- OHTSUBO, M., YOSHIMURA, A., WADA, S-I. and YONG, R.N.: Particle interaction and rheology of illite-iron oxide complexes. *Clays Clay Minerals*, 39, 1991, pp.347-354.
- PUGH, R.J.: Selective coagulation of colloidal mineral particles. In: J.S. Laskowski and J. Ralston (Editors), *Colloid Chemistry in Mineral Processing*. Elsevier, Amsterdam, 1992, pp: 243-276.
- RYDE, N. and MATIJEVIC, E.: Kinetics of heterocoagulation. Part 4 – Evaluation of absolute coagulation rate constants using a classical light scattering technique. *J. Chem. Soc. Faraday Trans.*, 90, 1994, pp.167-171.
- ŠKVARLA, J.: Detection of heterocoagulation-stability transition in binary colloidal system by electrophoretic light scattering. Silica-silica/aminopropyl system. *Colloids Surfaces*, 110, 1996a, pp.135-139.
- ŠKVARLA, J.: Evaluation of mutual interaction in binary mineral suspension by means of electrophoretic light scattering (ELS). *Int. J. Miner. Process.*, 48, 1996b, pp.95-109.
- WANG, Y., FORRSBERG, E. and PUGH, R.J.: The influence of pH on the high gradient magnetic separation of < 10 μm particles of hematite and quartz. *Int. J. Miner. Process.*, 36, 1992, pp.93-105.
- WARE, B.R. and HAAS, D.D.: Electrophoretic light scattering in: *Fast Methods in Physical Biochemistry and Cell Biology* (R.I. Sha'afi and S.M. Fernandez eds.), Elsevier, Amsterdam, 1983, Chapter 8, pp.174-220.
- WEINER, B.B., TSCHARNUTER, W.W. and FAIRHURST, D.: Zeta potential: A new approach. *Canadian Mineral Analysts Meeting*, September 8-12, Winnipeg Manitoba, Canada, 1993.
- WIESE, G.R. and HEALY, T.W.: Coagulation and electrokinetic behavior of TiO₂ and Al₂O₃ colloidal dispersions. *J. Colloid Interface Sci.*, 51, 1975a, pp.427-433.
- WIESE, G.R. and HEALY, T.W.: Adsorption of Al(III) at the TiO₂-H₂O interface. *J. Colloid Interface Sci.*, 51, 1975b, pp.434-442.
- WIESE, G.R. and HEALY, T.W.: Heterocoagulation in mixed TiO₂-Al₂O₃ dispersions. *J. Colloid Interface Sci.*, 52, 1975c, pp.452-457.
- WIESE, G.R. and HEALY, T.W.: Solubility effect in TiO₂ and Al₂O₃ colloidal dispersions. *J. Colloid Interface Sci.*, 52, 1975d, pp.458-467.
- WILSON, B.A. and CRIMP, B.J.: Prediction of composite colloidal suspension stability based upon the Hogg, Healy and Fuerstenau interpretation. *Langmuir*, 9, 1993, pp.2836-2843.
- YONG, R.N. and OHTSUBO, M.: Interparticle action and rheology of kaolinite-amorphous iron hydroxide (ferrihydrite) complexes. *Appl. Clay Sci.*, 2, 1987, pp.63-81.
- XU, R.: Methods to resolve mobility from electrophoretic laser light scattering measurements. *Langmuir*, 9, 1993, pp.2955-2962.